Influence of Pixel Size on Quantification of Airway Wall Thickness in Computed Tomography

Tobias Achenbach, MD, Oliver Weinheimer, PhD,* Christoph Dueber,* and Claus Peter Heussel, MD†*

Objectives: The purpose of this study was to determine the point where a further decrease in voxel size does not result in better automatic quantification of the bronchial wall thickness by using 2 different assessment techniques.

Materials and Methods: The results from the commonly used full-width-at-half-maximum (FWHM) principle and a new technique (integral-based method [IBM]) were compared for thin-section multidetector computed tomography (MDCT) data sets from an airway phantom containing 10 different tubular airway phantoms and in a human subsegmental bronchus in vivo. Correlation with the actual wall thickness and comparison of the wall thicknesses assessed for different voxel sizes were performed, and the image resolutions were also compared subjectively.

Results: The relative error ranged from 0% (biggest phantom) to 330% (smallest phantom, biggest field of view, smaller matrix, and FWHM). Using IBM, the maximum relative error was 10% in the same setting. For FWHM, the improvement was marginal for most settings with a pixel spacing less than $0.195 \times 0.195 \times 0.8$ mm; however, it still decreases the relative error from 290% to 273.6% for a wall thickness of 0.3 mm and a pixel spacing of $0.076 \times 0.076 \times 0.8$ mm.

Conclusions: (1) Using a special technique such as IBM to account for computed tomography's blurring effect in assessing airway wall thickness had the greatest impact on correct quantification. (2) The visual impression and the automatic quantification using the FWHM technique improved marginally by decreasing the voxel size to less than $0.195 \times 0.195 \times 0.8$ mm. (3) The FWHM technique as a model for visual quantification is not reliable for airway wall thicknesses less than 1.5 mm.

Key Words: computed tomography, airway, quantification

(*J Comput Assist Tomogr* 2009;33: 725–730)

Resolution is one of the crucial parameters in computed tomographic (CT) imaging. In a high-contrast organ such as the lung, resolution is the limiting factor for detailed imaging of morphological features, for example, for quantifying small structures such as nodules or the bronchial wall. In the last decade, resolution was improved down to submillimeter levels in the z-axis through the clinical implementation of multidetector CT scanners, and the effects on resolution were explored for different settings.[1] In the z-/y-plane, however, no relevant developments reached daily clinical routine. Current CT scanners offer the technical possibility of increasing the image matrix of 512^2 to 1024^2. In combination with a reduction in the field of view (FOV), the in-plane resolution can be increased down to an x-y pixel size of, for example, 0.2 mm. Only few studies have dealt with this matter up to now, and most of them analyzed the coronary arteries. The group of Wildberger found a benefit of small FOV sizes for detecting coronary calcifications that even influenced the risk stratification for further cardiac events.[2] Comparable results were presented by Hong et al[3] who showed a higher sensitivity for detecting calcifications by using smaller FOVs, and Herzog et al[4] reported an increased image quality, but diagnostic accuracy remained constant.

These studies underlined the fact that the information from the raw data is not fully used in routine diagnostic workup. However, physical limitations limit the maximum resolution. The influences of varying in-plane resolution on diagnostic accuracy in lung parenchyma and airway imaging have not been examined in detail up to now.

In a previous trial, we compared 2 different voxel sizes ($0.19 \times 0.19 \times 0.9$ and $0.35 \times 0.35 \times 0.9$ mm^3) and found that the dedicated integral-based method (IBM) gave better accuracy for airway morphometry than did the commonly used technique known as full width at half maximum (FWHM). For wall thicknesses of 1 mm or less, the relative error was smaller for the decreased voxel size. The intention of the current study was to determine the point where further reduction of the voxel size does not further increase the quantification accuracy using an airway phantom.

MATERIALS AND METHODS

Ten different high-precision silicon tubes for laboratory use (Deutsch & Neumann, Berlin, Germany) were aligned in parallel to the z-axis with the help of the gantry's laser light. Inner diameters, wall thickness, and physical density of the tubes were known and are presented in Tables 1 and 2. The inner diameter ranged from 2 to 4 mm, and the wall thickness ranged from 0.3 to 2.5 mm. All tubes were examined in the same way by using a 64-slice CT scanner (Brilliance 64; Philips Medical Solution, Netherlands). Scan parameters were as follows: collimation, 64×0.625 mm; tube current, 100 mA; tube voltage, 120 kV; rotation time, 0.5 s; and pitch, 0.9. Reconstruction parameters were as follows: slice thickness, 1 mm; increment, 0.8 mm; and filter, L (edge enhancing).

The images were analyzed with a dedicated scientific in-house software called YACTA, which has been described previously.[5] In brief, the software, which is written in C++, processes the density profile of 128 rays sent out virtually from a central luminal point derived from a skeleton axis. The FWHM technique identifies the airway borders at 50% of the gray-level maximum, thus overestimating its thickness each time. By applying the IBM, CT's blurring effect, by which especially small objects are enlarged, is minimized by virtually adapting the integral under the gray-level profile or reversing the blurring effect. To avoid minimal influences that are derived from different sites of the phantoms on the physical matrix grid of the scanner, all measurements were performed on a

From the *Department of Diagnostic and Interventional Radiology, Johannes Gutenberg University, Mainz, and †Thoraxklinik, University Hospital Heidelberg, Heidelberg, Germany.

Received for publication May 22, 2008; accepted October 7, 2008.

Reprints: Tobias Achenbach, MD, Department of Diagnostic and Interventional Radiology, Johannes Gutenberg University, Langenbeckstrasse 1, 55101 Mainz, Germany (e-mail: achenbac@uni-mainz.de).

This study was partially supported by the Deutsche Forschungsgesellschaft (German Research Foundation) FOR474-2 and AstraZeneca, Lund, Sweden.

TABLE 1. Assessed Wall Thicknesses (in Millimeters) of All Phantoms for All Different Reconstruction Settings

	Matrix of 512				Matrix of 1024				Real Wall Thickness	Phantom No
FWHM	2.58	2.53	2.52	2.51	2.53	2.52	2.52	2.51	2.5	1
	2.15	2.06	2.05	2.04	2.06	2.04	2.04	2.00	2.0	2
	2.10	2.03	2.01	2.01	2.03	2.01	2.00	2.00	2.0	3
	1.73	1.60	1.56	1.56	1.59	1.56	1.56	1.55	1.5	4
	1.73	1.60	1.56	1.56	1.59	1.56	1.57	1.55	1.5	5
	1.53	1.32	1.27	1.25	1.30	1.27	1.25	1.25	1.0	6
	1.52	1.30	1.23	1.22	1.29	1.23	1.22	1.21	1.0	7
	1.40	1.12	1.03	1.01	1.10	1.03	1.01	1.00	0.5	8
	1.43	1.15	1.06	1.04	1.12	1.06	1.03	1.03	0.4	9
	1.29	1.28	1.16	1.13	1.25	1.17	1.13	1.12	0.3	10
IBM	2.53	2.50	2.51	2.50	2.51	2.50	2.50	2.52	2.5	1
	1.99	1.99	1.97	1.97	1.98	1.97	1.97	1.96	2.0	2
	1.98	1.99	2.00	1.98	1.99	1.99	1.98	1.97	2.0	3
	1.48	1.49	1.49	1.49	1.49	1.49	1.49	1.49	1.5	4
	1.48	1.48	1.47	1.47	1.48	1.47	1.47	1.47	1.5	5
	1.08	1.06	1.03	1.03	1.04	1.03	1.02	1.01	1.0	6
	1.00	1.02	1.00	1.00	1.01	1.00	1.00	1.00	1.0	7
	0.55	0.54	0.54	0.53	0.54	0.54	0.53	0.54	0.5	8
	0.41	0.42	0.41	0.41	0.41	0.41	0.41	0.40	0.4	9
	0.27	0.30	0.30	0.29	0.30	0.29	0.29	0.28	0.3	10
Pixel edge length, mm	0.703	0.391	0.195	0.152	0.352	0.195	0.098	0.076		
FOV, mm	360	200	100	50	360	200	100	50		

TABLE 2. Relative Error (in Percentage) of the Assessed Wall Thickness of All Phantoms for All Different Reconstruction Settings

	Matrix of 512				Matrix of 1024				Real Wall Thickness	Phantom No
FWHM	3.2	1.2	0.8	0.4	1.2	0.8	0.8	0.4	2.5	1
	7.5	3	2.5	2	3	2	2	0	2.0	2
	5	1.5	0.5	0.5	1.5	0.5	0	0	2.0	3
	15.33	6.67	4	4	6	4	4	3.33	1.5	4
	15.33	6.67	4	4	6	4	4.67	3.33	1.5	5
	53	32	27	25	30	27	25	25	1.0	6
	52	30	23	22	29	23	22	21	1.0	7
	180	124	106	102	120	106	102	100	0.5	8
	257.5	187.5	165	160	180	165	157.5	157.5	0.4	9
	330	326.7	286.7	276.7	316.7	290	276.7	273.3	0.3	10
IBM	1.2	0	0.4	0	0.4	0	0	0.8	2.5	1
	0.5	0.5	1.5	1.5	1	1.5	1.5	2	2.0	2
	1	0.5	0	1.0	0.5	0.5	1	1.5	2.0	3
	1.33	0.67	0.67	0.67	0.67	0.67	0.67	0.67	1.5	4
	1.33	1.33	2	2.00	1.33	2	2	2	1.5	5
	8	6	3	3.00	4	3	2	1	1.0	6
	0	2	0	0	1	0	0	0	1.0	7
	10	8	8	6	8	8	6	8	0.5	8
	2.5	5	2.5	2.5	2.5	2.5	2.5	0	0.4	9
	10	0	0	3.33	0	3.33	3.33	6.67	0.3	10
Pixel edge length, mm	0.703	0.391	0.195	0.152	0.352	0.195	0.098	0.076		
FOV, mm	360	200	100	50	360	200	100	50		

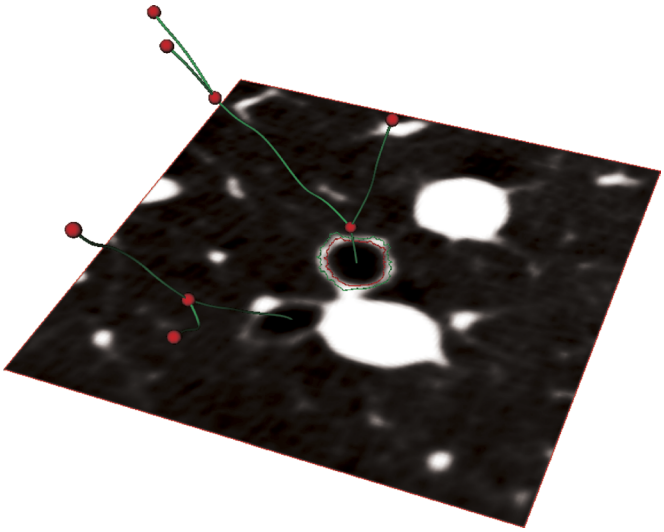

FIGURE 1. Three-dimensional visualization of a subsegmental bronchial branching (points and lines) in relation to an orthogonal zoomed CT image. The green lines demark the central line of the airways derived by automatic skeletonization. The red dots represent branching or end points, respectively. The inner (red) and outer (green) borderlines of the airway wall as assessed are marked.

real 3-dimensional basis, additionally abolishing undetected deflection from the z-axis (Fig. 1). For measurements on the density profiles, the 2 techniques, FWHM and IBM, were used. We additionally assessed the bronchial wall thickness of a human subsegmental airway on a CT data set derived from clinical routine. A standard thin-collimated multidetector computed tomography (MDCT) was used (collimation, 64 × 0.625 mm; tube current, 120 mA; tube voltage, 120 kV; and pitch, 0.9). Multiple reconstructions from the same raw data were calculated using the same FOVs and matrices applied to the phantoms (minimum and 100-, 200-, and 360-mm FOV—each FOV reconstructed with both matrices of $512^2$and 1024^2). This varied the pixel size from 0.7 to 0.076 mm^2. For statistical evaluation, SPSS 11 (SPSS, Chicago, IL) was used. Correlation coefficients and simple scatter diagrams were calculated.

RESULTS

The assessed wall thicknesses and the calculated relative errors for each airway phantom and every reconstruction setting are shown in detail in Tables 1 (wall thicknesses) and 2 (relative errors). For the largest airway phantom with a wall thickness of 2.5 mm, the assessed wall thickness on the images with a 512^2 matrix and an FOV of 360 mm (FWHM/IBM) was 2.58 mm/2.53 mm and for the smallest FOV of 50 mm was 2.51 mm/2.51 mm. The relative error for an FOV of 360 mm (FWHM/IBM) was 3.2%/1.2% and for the smallest FOV of 50 mm was 0.4%/0%. For the same airway phantom, the assessed wall thickness on the images with a 1024^2 matrix and an FOV of 360 mm (FWHM/IBM) was 2.53 mm/2.51 mm and for the smallest FOV of 50 mm was 2.51 mm/2.52 mm. The relative error for the FOV of 360 mm (FWHM/IBM) was 1.2%/0.4% and for the smallest FOV of 50 mm was 0.4%/0.8%.

For the smallest airway phantom with a wall thickness of 0.3 mm, the assessed wall thickness on the images with a 512^2 matrix and an FOV of 360 mm (FWHM/IBM) was 1.29 mm/0.27 mm and for the smallest FOV of 50 mm was 1.13 mm/0.29 mm. The relative error for an FOV of 360 mm (FWHM/IBM) was 330%/10% and for the smallest FOV of 50 mm was 276.67%/3.33%. For the same airway phantom, the assessed wall thickness on the images with a 1024^2 matrix and an FOV of 360 mm (FWHM/IBM) was 1.25 mm/0.3 mm and for the smallest FOV of 50 mm 1.12 mm/0.28 mm. The relative error for an FOV of 360 mm (FWHM/IBM) was 316.67%/0% and for the smallest FOV of 50 mm was 273.33%/6.67%. The largest pixel spacing was 0.703 × 0.703 × 0.8 mm^3, and the smallest pixel spacing was 0.076 × 0.076 × 0.8 mm^3 (Figs. 2 and 3). In vivo, the selected bronchus of the lower lobe using FWHM was 1.24 mm for the smallest pixel size and 1.76 mm for the largest pixel size, showing a difference of 0.52 mm and 41.9%, respectively. The in vivo measurement of the same bronchus using the IBM differed between 0.41 and 0.39 mm, corresponding to a difference of 0.02 mm or 4.9% (Table 3).

The subjective analysis showed a clear improvement in resolution for images reconstructed with a matrix of 512^2 and an FOV of 100 and a matrix of 1024^2 and an FOV of 200, respectively, compared with that for images with larger voxel sizes such as the clinical standard situation (matrix, 512^2 and FOV, 360), which showed obvious stairs of the bronchus wall. The improvement provided by smaller voxel sizes was only visible by carefully scrutinizing and comparing them with the enlarged images (Fig. 4).

DISCUSSION

Using a simple study design, we compared the actual wall thickness of an idealized airway phantom with the wall thicknesses assessed by 2 different automated methods (FWHM and IBM) for different pixel sizes as determined by the FOV and the option to vary the image matrix from 512^2 to 1024^2 (although 768^2 is also technically available). We use the term *pixel* deliberately as we improve resolution in the x-/y-plane and keep the edge length of the voxel along the z-axis constant to a state-of-the-art pulmonary CT with 0.8 mm. For the dedicated IBM, the influence of decreasing pixel sizes was minor. Comparing the largest pixel size of 0.703 × 0.703 × 0.8 mm^3 to the smallest pixel size of 0.076 × 0.076 × 0.8 mm^3,

the relative error for the smallest phantom with a 0.3-mm wall thickness was 10% and 7%, respectively. These results are surprisingly good: However, this method was especially designed to eliminate the sampling effect hampering the measurement of small structures in CT images. More important for clinical radiology are the results of the method working with the FWHM principle as this method somehow models the radiologist's visual, subjective, and manual technique of measuring small structures on CT. Human readers of images will instinctively search for the objects' border halfway between the maximum and the minimum of a gray-level profile, which is not correct for small structures because of CT's blurring effect. By decreasing the pixel size, we found a successive improvement in the accuracy of the FWHM method, particularly for phantoms with wall thicknesses of 1.5 mm and smaller. However, even the smallest FOV combined with the 1024 matrix showed a relative error of more than 273% when measuring the smallest phantom with a wall thickness of 0.3 mm. Nevertheless, doubling the matrix or minimizing the FOV produced acceptable results, with relative errors of 21% to 30% for distances of 1 mm and more, which is the most important scale for daily clinical routine, in our opinion. These results are in line with those of studies on imaging of coronary arteries.[2,3] Our findings also indicate that to gain an impression of smaller objects—either within the lung, which is a high-contrast organ, or possibly other organs—and especially if the object's size is of interest or even must be quantified—special reconstructions with minimized FOVs should be used. Further quantification of distances smaller than 1 mm should be avoided unless special techniques such as the IBM are available. A similar conclusion was found in another airway phantom study conducted by Saba et al[6]; however, here, the radius, and not the airway wall, was measured, and the phantoms were less anthropomorphic, with wall thicknesses of between 1.16 and 3.05 mm. Earlier empirical studies aiming to subjectively describe the morphological high resolution computed tomography HRCT features of pulmonary nodules recommended higher resolutions, too.[7] The highest reasonable resolution for this subjective setting was reached by using voxel sizes of about $0.195 \times 0.195 \times 0.8$ mm—obviously a crucial border, where the maximum resolution of the CT raw data is exhausted. As simple as this message is, the clinical impact represents an unknown as the standard FOV is normally beyond the body surface, except in special examinations such as cardiac CT or CT of the sphenoid bone. However, according to our in vivo test, relative errors presumably must be higher: Using the IBM, the bronchus showed a wall thickness in vivo of approximately 0.4 mm, and using the FWHM technique, it showed a wall thickness in vivo of 1.24 to 1.76 mm. In the

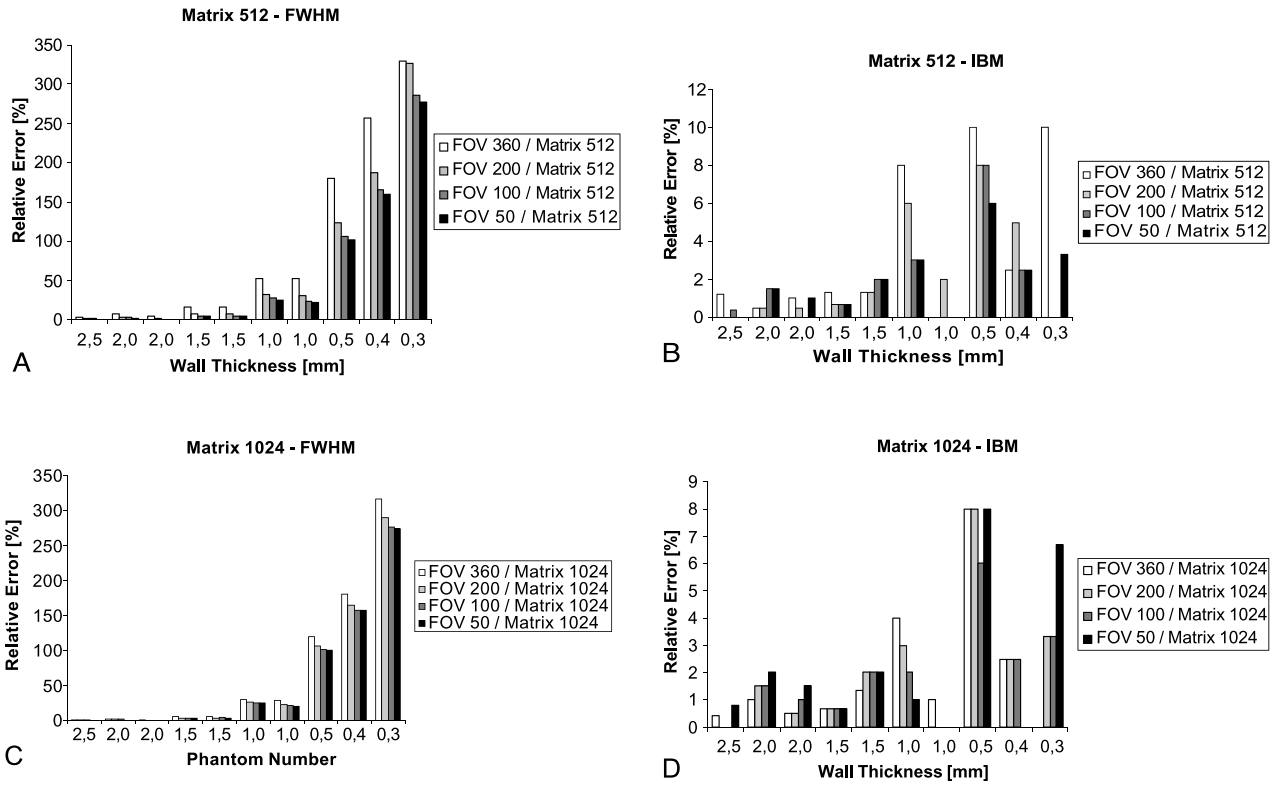

FIGURE 2. A, B, Vertical bar chart of the relative errors of wall thickness quantification (matrix 512) shows high relative errors in the small phantoms (y-axis) using the FWHM technique (A) and clear improvement by using the IBM (B). Note the decrease in the relative error when using smaller FOVs in FWHM, producing acceptable results for wall thicknesses of about 1 to 1.5 mm (phantom number 5 to 7). Note the different scale of the y-axis. C, D, Vertical bar chart of the relative errors of wall thickness quantification (matrix, 1024) shows high relative errors in the small phantoms (y-axis) using the FWHM technique (C) and clear improvement by using the IBM (D). As in panel A, decreasing FOV sizes result in smaller errors (C), which are still unacceptably high for wall thicknesses less than 0.5 mm. Note the different scale of the y-axis.

TABLE 3. In Vivo Assessment of a Subsegmental Bronchus for All Reconstruction Settings With Both Assessment Techniques

	Matrix of 512				Matrix of 1024			
FWHM	1.76	1.39	1.28	1.26	1.37	1.27	1.24	1.24
IBM	0.41	0.40	0.41	0.39	0.40	0.40	0.40	0.41
FOV, mm	360	200	100	50	360	200	100	50

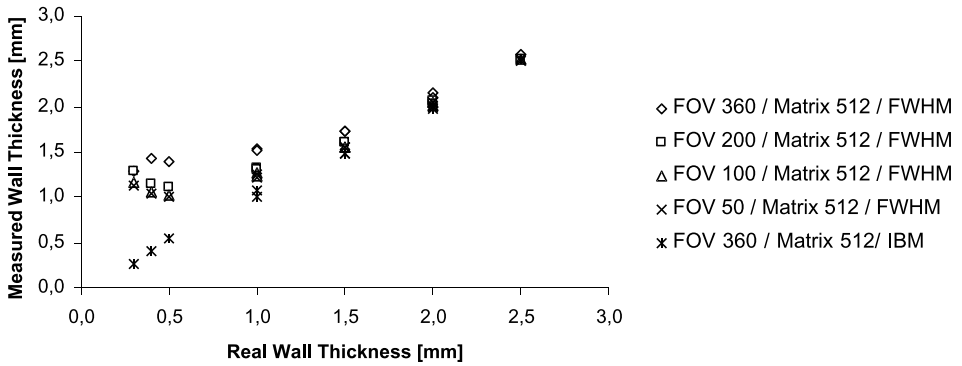

FIGURE 3. Correlation of the actual wall thickness and the measured wall thickness of all phantoms using the FWHM technique and a matrix of 512 with decreasing FOVs compared with those using the IBM (asterisks). However, using the lowest resolution IBM does not result in increasing overestimation with decreasing airway wall thickness (note the consecutive gap for phantoms with wall thicknesses of 1 mm or less).

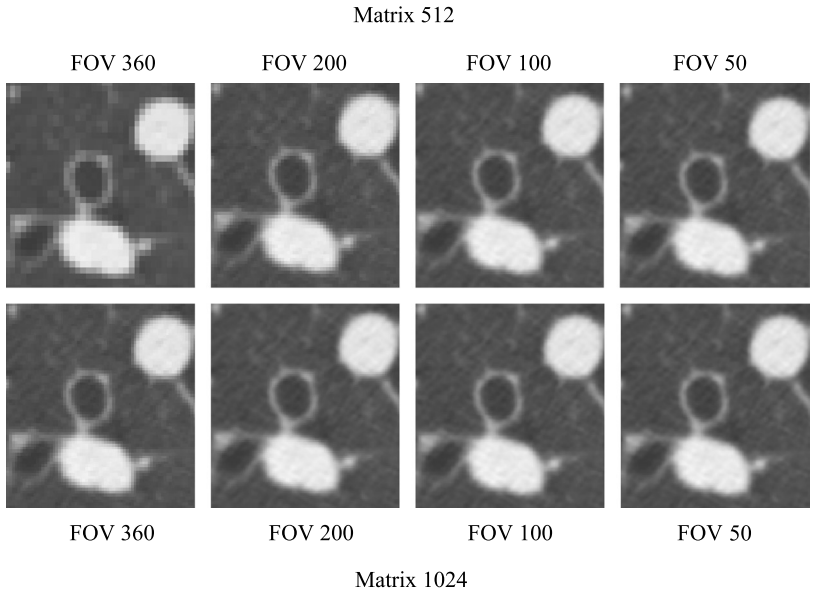

FIGURE 4. Screen shots of all reconstruction settings for the subsegmental human bronchus. Note the smoother definition of the bronchial wall with decreasing FOV compared with that of the standard situation (FOV, 360 and matrix, 512^2). Shrinking the pixel size to less than 0.195^2 brings only very slight improvement in sharpness.

phantom, however, with a known wall thickness of 0.4 mm, wall thicknesses of between 1.03 and 1.43 mm were measured using the FWHM technique. A possible explanation for this gap is the missing lung parenchyma around the phantom. A pathological-radiological correlation would be mandatory to clarify this point.

Our study does not examine the effect that different reconstruction algorithms have on quantification. Dougherty and Newman[8] described the effects in detail and demonstrated that sharper kernels reduced the blurring effect, thus reducing the overestimation of the FWHM technique. Integral-based method accounts for the reconstruction algorithms by gradually changing the modification of the integral.

Most diagnoses can presumably be made at standard resolution, but our study has demonstrated that a smaller pixel size is beneficial for visually assessing smaller airways. Particularly those settings in which it is crucial for diagnosis to quantify small structures or assess subtle morphological features (eg, lung nodules, interstitial lung diseases, or pneumonia) could be explored to determine whether diagnostic accuracy is higher when using a small pixel size—either derived by higher matrices or, if technically impossible, a focused FOV or a combination of the two techniques.[9] Different scientific tasks must be carried out to judge the clinical impact of higher resolutions: for example, the investigation of standard values of bronchial wall thickness. Our study provides a basis for these next steps.

CONCLUSION

When high accuracy is required for quantifying the bronchial wall thickness on lung CT, pixel sizes should be reduced down to $0.195 \times 0.195 \times 0.8$ mm to produce high-resolution images, especially for expected wall thicknesses of 1.5 mm and smaller. Nevertheless, for measuring even smaller objects, the assessment technique is the crucial factor as it compensates for the influence of the CT-specific spread function. In this case, advanced techniques beyond the FWHM principle such as the IBM are recommended.

REFERENCES

1. Goo JM, Tongdee T, Tongdee R, et al. Volumetric measurement of synthetic lung nodules with multi-detector row CT: effect of various image reconstruction parameters and segmentation thresholds on measurement accuracy. *Radiology.* 2005;235:850–856.
2. Mahnken AH, Muhlenbruch G, Koos R, et al. Influence of a small field-of-view size on the detection of coronary artery calcifications with MSCT: in vitro and in vivo study. *Eur Radiol*. 2006;16:358–364.
3. Hong C, Pilgram TK, Zhu F, et al. Coronary artery calcification: effect of size of field of view on multi-detector row CT measurements. *Radiology.* 2004;233:281–285.
4. Herzog C, Nguyen SA, Savino G, et al. Does two-segment image reconstruction at 64-section CT coronary angiography improve image quality and diagnostic accuracy? *Radiology.* 2007;244:121–129.
5. Weinheimer O, Achenbach T, Bletz C, et al. About objective 3-d analysis of airway geometry in computerized tomography. *IEEE Trans Med Imaging*. 2008;27:64–74.
6. Saba OI, Hoffman EA, Reinhardt JM. Maximizing quantitative accuracy of lung airway lumen and wall measures obtained from x-ray CT imaging. *J Appl Physiol*. 2003;95:1063–1075.
7. Seemann MD, Staebler A, Beinert T, et al. Usefulness of morphological characteristics for the differentiation of benign from malignant solitary pulmonary lesions using HRCT. *Eur Radiol*. 1999;9:409–417.
8. Dougherty G, Newman D. Measurement of thickness and density of thin structures by computed tomography: a simulation study. *Med Phys*. 1999;26:1342–1348.
9. Honda O, Sumikawa H, Johkoh T, et al. Computer-assisted lung nodule volumetry from multi-detector row CT: influence of image reconstruction parameters. *Eur J Radiol*. 2007;62:106–113.